6282 *Biochemistry* **2010,** *49,* 6282–6289
DOI: 10.1021/bi100753s

BIOCHEMISTRY
including biophysical chemistry & molecular biology
Article

The Oxidoreductase Behavior of Protein Disulfide Isomerase Impedes Fold Maturation of Endoplasmic Reticulum-Processed Proteins in the Pivotal Structure-Coupled Step of Oxidative Folding: Implications for Subcellular Protein Trafficking[†]

Veronica Gonzalez,[‡] Rituraj Pal,[‡] and Mahesh Narayan*

Department of Chemistry, University of Texas at El Paso, El Paso, Texas 79968
[‡]*These authors contributed equally to this work*

Received May 12, 2010; Revised Manuscript Received June 8, 2010

ABSTRACT: Protein disulfide isomerase (PDI), the chief endoplasmic reticulum (ER) resident oxidoreductase chaperone, is known to catalyze the maturation of disulfide bond-containing proteins primarily through oxidation and isomerization functions. The rate-determining step in the oxidative regeneration path of disulfide bond-containing proteins generally couples chemical thiol−disulfide-exchange reactions to a physical conformational folding reaction. We have determined the impact of PDI and its subdomains on the rate-determining step in ribonuclease A folding and on the physical structure-forming step of select ER-processed proteins including RNase A. This was facilitated through application of a novel chemical tool to exclusively populate native disulfide-containing intermediates in unstructured forms. The described biochemical inroad permits a deconvoluted study of the physical half-process in the rate-determining step from its chemical counterpart. Analysis of folding kinetics of RNase A and other proteins reveals that the highly evolved oxidoreductase activity of PDI masks its chaperone-like activity, impedes conformational folding of ER-processed proteins, and limits its potential to accelerate the rate-determining step in oxidative regeneration. Implications of the heretofore unknown and anomalous self-limiting behavior of PDI are discussed in the context of oxidative maturation and misfolding *in vivo*.

Oxidative protein folding is characteristic of many proteins that are secreted outside the cell or are membrane-bound and possess disulfide bonds (*1*−*4*). It is a composite process because it involves the chemical formation of the native set of disulfide bonds from the fully reduced polypeptide that is coupled to a physical conformational folding reaction to obtain the native, biologically active structure (*1*−*3*). Proteins required to oxidatively fold are processed (mature) within the endoplasmic reticulum (ER),[1] which facilitates disulfide bond formation because of a favorable redox potential (*4*).

A typical oxidative folding reaction comprising the regeneration of bovine pancreatic ribonuclease A (RNase A) is shown in Figure 1. During its regeneration from the fully reduced state (R), 28 one-disulfide (1S), 210 two-disulfide (2S), 420 three-disulfide (3S), and 104 scrambled (i.e., non-native) four-disulfide (4S) containing intermediates are formed (Figure 1) (*5*−*8*). Additionally, two native-like species accumulate in the rate-determining step (RDS) of the reaction. These are des [40−95] and des [65−72] which possess native-like structure and lack the (40−95) and (65−72) disulfide bond, respectively (*9*, *10*). These structured intermediates (also referred to as 3S*) are then oxidized to form N (Figure 1) (*1*). The formation of 3S* from 3S is rate-determining because it involves the formation of two native disulfide bond-containing structured intermediates from an isomer ensemble of 420 unstructured intermediates which mostly contain non-native disulfide bonds, making the search for those two (3S*) species statistical and hence time-consuming; in RNase A this search is compounded by a slow conformational folding process. These two processes are elaborated below.

The rate-determining step (RDS) in most oxidative folding pathways, including that of RNase A, is composed of chemical and physical half-processes (*5*−*7*). The chemical half of the RDS in RNase A involves thiol−disulfide exchange reactions to populate an unstructured intermediate with native disulfide bonds ($3S_{native}$) from its non-native disulfide bond-containing isomers ($3S_{non\text{-}native}$) [($3S_{non\text{-}native}$ → $3S_{native}$) (Figure 2). For example, consider the formation of unstructured des (40−95) from its 419 unstructured 3S isomers (Figure 2B). These isomers must chemically reshuffle to produce an unstructured intermediate ($3S_{non\text{-}native}$) that is one step away from a chemical reshuffling reaction to produce unstructured des (40−95). Such a $3S_{non\text{-}native}$ species will contain two native disulfide bonds (solid lines) and one non-native disulfide bond (dotted line). Similar scenarios are

[†]M.N. acknowledges start-up/seed money from UTEP.
*To whom correspondence should be addressed. Phone: (915) 747-6614. Fax: (915) 747-5748. E-mail: mnarayan@utep.edu.

[1]Abbreviations: ER, endoplasmic reticulum; N, native protein/species; R, fully reduced protein/species; PDI, protein disulfide isomerase; DTT^{red}, reduced dithiothreitol; DTT^{ox}, oxidized dithiothreitol; RNase A, bovine pancreatic ribonuclease A; ALAC, α-lactalbumin; RDS, rate-determining step; des [40, 95] RNase A, a structured intermediate of ribonuclease A lacking the disulfide bond between the cysteine residues denoted in the brackets; des [65−72] RNase A, a structured intermediate of ribonuclease A lacking the disulfide bond between the cysteine residues denoted in the brackets; 1S, one disulfide bond-containing isomer ensemble of folding intermediates; 2S, two disulfide bond-containing isomer ensemble of folding intermediates; 3S, three disulfide bond-containing isomer ensemble of folding intermediates; 4S, four disulfide bond-containing isomer ensemble of folding intermediates; $3S_{native}$, an unstructured intermediate that contains three native disulfides and is poised to fold; $3S_{non\text{-}native}$, an unstructured intermediate that contains three disulfide bonds of which only one is non-native (such an intermediate is one chemical reshuffling step away from forming $3S_{non\text{-}native}$); 3S*, a structured three disulfide bond-containing intermediate (such as des [40−95] and des [65−72]) formed by conformational folding of $3S_{native}$.

 Published on Web 06/22/2010

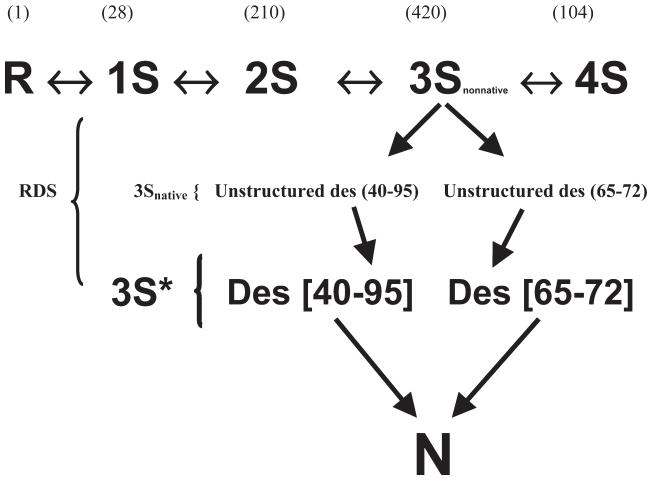

FIGURE 1: Regeneration scheme of RNase A (pH 8, 25 °C). R, 1S, 2S, 3S, and 4S are unstructured intermediates (the numbers above each species refer to the number of existing isomers when no mixed disulfide-containing intermediates are present, such as when using glutathione as the redox reagent). Des [40−95] and des [65−72] are native-like three disulfide bond-containing intermediates and are also referred to as the 3S* species. They are formed from their unstructured native disulfide bond-containing precursors (collectively known as $3S_{native}$) by a conformational folding reaction in the rate-determining step (RDS; 3S → 3S*). N is the native protein and is eventually formed by oxidation of nativelike 3S* species.

depicted for unstructured des (65−72) in Figure 2C. In both cases, the statistical dependence of the formation of unstructured des (40−95) and des (65−72) from 419 isomers prolongs the process and contributes to the step becoming rate-determining.

The physical half of the RDS involves a conformational folding event; viz., the native disulfide bond-containing intermediate ($3S_{native}$) conformationally folds to generate a native or native-like structure (3S*) that preserves newly acquired native disulfide bonds by preventing access to chemical exchange (*5*−*7*). The physical conformational folding reaction is pivotal to the oxidative folding process because it removes the newly structured intermediate from the quasi-equilibrium pool of unstructured intermediates that are prone to unfruitful oxidation, reduction, and reshuffling reactions (Figure 1) (*8*, *9*).

Thus, $3S_{non\text{-}native}$ and $3S_{native}$ comprise the chemical half of the rate-determining step of the regeneration pathway. $3S_{native}$ and 3S*, which contain the same set of native disulfide bonds, comprise the physical half of the rate-determining step of the regeneration pathway. Taken together, these three species constitute the RDS of the oxidative folding pathway.

Importantly, the physical conformational folding half of the RDS competes with its chemical counterpart (thiol−disulfide exchange reactions) (Figure 2) (*5*−*7*, *11*, *12*). The forward conformational folding reaction ($3S_{native}$ → 3S*) must outcompete back-reshuffling reactions ($3S_{native}$ → $3S_{non\text{-}native}$) if a structured (native-like or native) species is to be formed (*10*, *13*).

In RNase A, proline isomerization slows conformational folding of both unstructured des (40−95) and unstructured des (65−72) to des [40−95] and des [65−72], respectively. Therefore, a major fraction of $3S_{native}$ species formed in each case reshuffles to its precursor non-native disulfide bond-containing isomer ($3S_{non\text{-}native}$) which can then reshuffle to any of the other 419 non-native disulfide bond-containing unstructured isomers (*13*). Thus, unless a $3S_{native}$ species can fold rapidly, it becomes susceptible to thiol−disulfide exchange. Another search through a series of time-consuming chemical exchange steps is then required to repopulate $3S_{native}$.

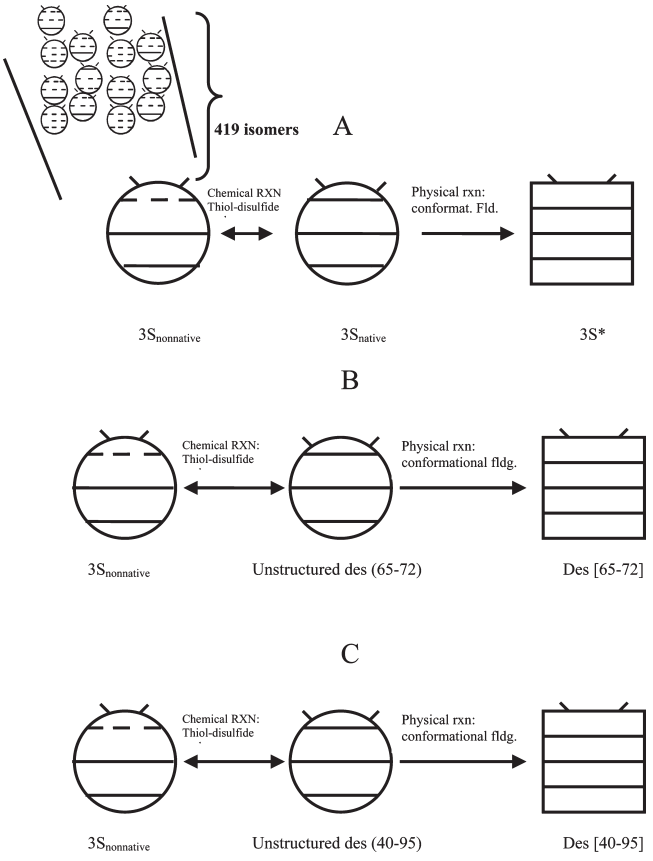

FIGURE 2: Representation of the rate-determining step (RDS) involving the formation of a structured species from its unstructured precursors via thiol disulfide exchange (chemical reaction) and confornmational folding (physical reaction) during oxidative folding. Dashed horizontal lines are non-native disulfide bonds in an unstructured intermediate, viz., $3S_{non\text{-}native}$; solid horizontal lines are native disulfide bonds in unstructured ($3S_{native}$) and structured intermediates (3S*). Vertical lines are thiols. A competition exists between reshuffling (isomerization) reactions [$3S_{native}$ ↔ $3S_{non\text{-}native}$] and the structure-forming step [$3S_{native}$ → 3S*]. (A) Generic pathway of a RDS involving the formation of 3S* via thiol−disulfide chemical reactions and a physical conformational folding reaction from its unstructured isomers. (B) Pathway showing the formation of des [65−72] from unstructured des (65−72) in RNase A RDS. (C) Pathway showing the formation of des [40−95] from unstructured des (40−95) in RNase A RDS.

The transient, poised-to-fold, nature of every $3S_{native}$ species makes the study of the RDS extremely difficult. This is because studies performed at a pH in the vicinity of the $3S_{native}$ thiol pK_a result in the reshuffling of $3S_{native}$ to $3S_{non\text{-}native}$; alternatively, $3S_{native}$ can also vanish by conformational folding to 3S*.

Note: In RNase A, at 15 °C, two other structured species accumulate (*6*). Des [58−110] and des [26−84] have thermal transitions of ~20 °C and hence do not populate the regeneration pathway at 25 °C.

Thus, every 3S* species has an unstructured precursor (viz., $3S_{native}$) that possesses the same identity of native disulfide bonds, except such an unstructured precursor is amenable to a forward physical folding reaction ($3S_{native}$ → 3S*) and/or a reverse chemical thiol−disulfide exchange reaction ($3S_{native}$ → $3S_{non\text{-}native}$). In other words, des [40−95], for example, transiently exists as des (40−95) until it folds or becomes reshuffled.

In other protein folding scenarios, the dependence of tertiary structure on a cofactor may impact conformational folding rates.

The competition between the "chemical" thiol−disulfide exchange reaction and the "physical" conformational folding reaction is unique to disulfide bond-containing proteins (*7*).

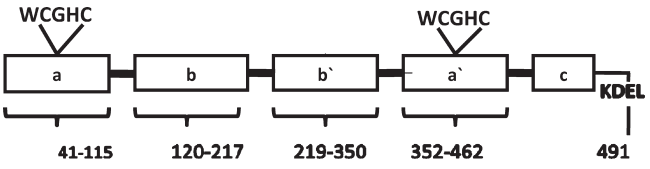

FIGURE 3: Schematic of protein disulfide isomerase (PDI) indicating the redox-active a and a′ domains and the hydrophobic b and b′ domains.

In vivo, oxidative protein folding is catalyzed by protein disulfide isomerase (PDI), which possesses oxidase and "shuffflase" activity using surface-exposed cysteine residues (Figure 3) (*12*, *14*−*17*). Although *in vitro* studies have demonstrated that PDI is able to accelerate oxidative folding reactions and catalyze the regeneration of multi-disulfide bond-containing proteins including RNase A (*18*), the impact of PDI and its domains on the pivotal structure-coupled step that immediately precedes maturation is yet unknown. Furthermore, even under surveillance by PDI, a large fraction of ER-processed proteins misfold and are trafficked to the proteosome (*4*). Given this scenario, and that PDI is the principal machinery charged with oxidative maturation of ER-processed proteins, it is of interest to examine its catalytic impact on both the structure-coupled step and the overall rate-determining step in oxidative folding, which is the subject of this study.

Heretofore, a study of the impact of PDI on the physical half of the RDS has not been reported; this is now possible by deconvoluting the chemical half of the RDS from its physical half and is essential to obtain a fundamental understanding of the impact of PDI on the microscopic steps of the RDS. Note that the RDS generally precedes maturation and export from the ER of disulfide bond-containing proteins. In this paper, we report a novel tool to exclusively populate native disulfide-containing intermediates in unstructured forms that are poised to fold or back-reshuffle to "futile" unfolded precursors. The described biochemical inroad permits a deconvoluted study of the physical half-process in the rate-determining step from its chemical counterpart and facilitates assessment of PDI's impact on this step and on ER trafficking in general. Our results reveal that though the chief ER-resident oxidoreductase successfully catalyzes the overall rate-determining step in RNase A regeneration, it hampers the piviotal structure-forming step in the maturation of RNase A and other ER-processed proteins. Furthermore, the chaperone and isomerase catalytic activities of PDI conflict in their ability to accelerate the formation of the native fold. The implications of these results on trafficking in the ER, protein misfolding, and the onset of neurodegenerative disorders are discussed.

MATERIALS AND METHODS

Materials. RNase A was purchased from Sigma and purified as previously described (*8*). Protein disulfide isomerase, null PDI, and ab, b′a′, and bb′ constructs were gifts from the laboratory of Prof. Arne Holmgren (Karolinska Institute, Sweden) and were expressed and purified as previously described (*19*). Oxidized and reduced dithiothreitol (DTT^{ox} and DTT^{red}, respectively) were purchased from Sigma and used without further purification. All other chemicals were of the highest grade commercially available.

Preparation of Fully Reduced RNase A. Fully reduced RNase A (R) was prepared by incubating native protein (10 mg/mL) in 6 M Gdn-HCl and 100 mM DTT^{red} (pH 8, 100 mM Tris-HCl, 1 mM EDTA) for a period of 2 h (*8*). The mixture was then repeatedly dialyzed against 50 mM acetic acid at 4 °C prior to lyophilization. The fully reduced protein was dissolved into 10 mM acetic acid to obtain a stock solution (5 mg/mL protein) that was kept frozen (−20 °C) until further use.

HPLC-isolated des [40−95] and des [65−72] were pooled and introduced into 6 M Gdn-HCl (pH 8, 100 mM Tris-HCl) as previously described (*13*). After 5 min, the pH of the solution was quenched by the addition of 20 μL of glacial acetic acid. The sample was then desalted using a G-25 column and lyophilized.

Reductive unfolding of native RNase A (5 mg/mL) was initiated by incubation of the protein in a buffer containing 100 mM DTT^{red} (pH 8, 100 mM Tris-HCl, 1 mM EDTA, 15 °C). Twenty hours after initiation of reduction, glacial acetic acid was added to reduce the pH to 3. The sample was desalted using a G-25 column, and native-like des [40−95] and des [65−72] were separated using strong cation-exchange chromatography as previously described (*9*).

Des [40−95] and des [65−72] were pooled and introduced into a pH 2 buffer (containing 50 mM acetic acid) as previously described (*13*). After 30 min of incubation, the solution was freeze-dried, and the lyophilized protein was introduced into a buffer containing 20 mM acetic acid (pH 3).

Oxidative Folding of RNase A. Aliquots of fully reduced RNase A (30 μM final concentration) were incubated into solutions (pH 8, 50 mM DTT^{ox}, 20 mM Tris-HCl, 1 mM EDTA, 25 °C) containing either 4 μM WT PDI, ab, bb′, or b′a′ domains. [Note: The use of DTT^{ox}, a weak oxidizing agent permits good kinetic control over regeneration rates and does not lead to the formation of mixed disulfide bonds. DTT^{red} is not initially added to the regeneration mixture because it is naturally formed upon oxidation of protein thiols to disulfides.] A control experiment that did not contain PDI or any of its domains was run in parallel (*8*). Aliquots from the regeneration mixture were withdrawn at several time points after the initiation of oxidative folding and subjected to a reduction pulse [application of 2 mM DTT^{red} for a period of 2 min (*9*)], before addition of glacial acetic acid (which reduced the pH to 3). Samples were desalted on a G-25 column prior to application on a C-18 column for reversed-phase chromatographic analysis.

The rate of regeneration of the native protein (N) was determined by integrating the areas of the peaks corresponding to the native protein (N), any structured intermediates (3S*), and the fully reduced protein (R) at each time point. The fractional increase in N was plotted as a function of time; the data were fitted to a single-exponential function to obtain the rate constant for the formation of N from R (*20*).

Impact of PDI on the Rate-Determining Step (3S → 3S) of RNase A Regeneration*. Lyophilized 3S was introduced into a folding buffer (30 μM protein, pH 8, 100 mM Tris-HCl). Aliquots were withdrawn and subjected to the reduction pulse at various time intervals (*13*). The reaction was quenched and then analyzed by HPLC as described above. In other experiments, the folding buffer contained either 4 μM WT PDI or its constructs.

The rate of formation of 3S* was determined from analysis of the peak areas corresponding to 3S* and $3S_{non\text{-}native}$ (R) as a function of time, as described previously (*20*).

Preparation of $3S_{native}$ (an Intermediate "Poised to Fold"). Des [65−92]and des [40−95] were obtained by strong cation-exchange fractional separation of a native RNase A that had been exposed to strongly reducing conditions as previously described, i.e., through reductive unfolding of the native protein (*6*, *13*).

Des [65−72] and des [40−95] were separately collected and desalted on a reversed-phase HPLC. They were then lyophilized before being separately introduced into solutions of dilute acetic acid (50 mM) as previously described to obtain unstructured des (65−72) and unstructured des (40−95), respectively (*13*).

Impact of PDI and Its Domains on the Structure-Forming Step of RNase A. $3S_{native}$ species (i.e., unstructured des (65−72) and unstructured des (40−95)) incubated at pH 2 in 50 mM acetic acid (and added HCl to bring the pH to 2) was introduced into a pH 8.2 solution (100 mM Tris-HCl, 1 mM EDTA) such that the final pH was 8 (30 μM protein). One minute later, the sample was subjected to a reduction pulse, as described above. All samples were then desalted and analyzed by reversed-phase HPLC (C18 column; 1%/min acetonitrile gradient).

The reduction pulse facilitates reduction of any unstructured intermediate such as unreacted $3S_{native}$ and its chemical isomerization product ($3S_{non\text{-}native}$) to the fully reduced protein (R) (*6*). These can be easily separated on a reversed-phase column as described above. The peak areas corresponding to 3S* and the fully reduced protein (R) are integrated to obtain the fraction of $3S_{native}$ that was able to physically fold and form 3S*.

The percent of $3S_{non\text{-}native}$ was calculated using the formula (*12*):

$$\%\ 3S_{non\text{-}native} = 100[\text{peak area (R)}]/[\text{peak area (R)} + \text{peak area } 3S*]$$

The percent of 3S* was determined by subtraction of the percent of $3S_{non\text{-}native}$ from 100.

In other experiments reduced wild-type PDI, null PDI, or each domain (at 4 μM, respectively) was introduced into the pH 8.2 buffer, prior to introduction of the 3S species.

Measurement of the impact of PDI, null PDI, and domains on the structure-forming step was assessed by measuring the areas under the HPLC peaks corresponding to fully reduced protein (R) and the structured 3S* species as previously described (*20*, *21*).

Preparation of Native Disulfide-Intact "Poised-to-Fold" Intermediates of Other ER-Processed Proteins. α-Lactalbumin (ALAC) was purchased from Sigma (>99.5% pure) and used without further purification. In order to retain native disulfide bonds and eliminate tertiary structure, ALAC (5 mg) was added to a pH 8 buffer (100 mM Tris-HCl) containing 5 mM EDTA and stored at 4 °C until further use (*22*). Under such conditions, Ca^{2+} is removed from the ALAC which results in a loss of tertiary structure and formation of a molten globule state (*22*). The Ca^{2+}-less form is called apo-ALAC.

C65AC72A RNase A, a three-disulfide intermediate of RNase A (available in the laboratory), was introduced (10 mg) into a buffer containing 4 M Gdn-HCl (pH 8, 100 mM Tris-HCl, 1 mM EDTA). Under these conditions, there is no evidence of tertiary structure even though native disulfide bonds persist (*10*, *13*). The solution was stored at 4 °C until further use.

Measurement of the Impact of WT Reduced PDI on the Structure-Forming Step of ALAC and C65AC72A RNase A. Apo-ALAC (5 mg/mL, pH 8, 100 mM Tris-HCl, 5 mM EDTA) was introduced into a folding buffer containing 20 mM Ca^{2+} such that the final protein concentration was 20 μM. Aliquots were withdrawn at 30 s, 1 min, and 2 min and immediately quenched using 20 μL of glacial acetic acid. Samples were analyzed by separation on a reversed-phase column and data processed as described above.

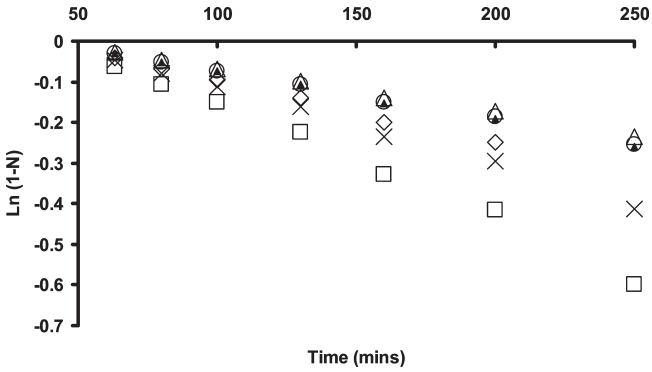

FIGURE 4: Plot of $\ln(1 - N)$ as a function of time. N is the fractional concentration of native RNase A regenerated. The regeneration conditions were (a) pH 8, 50 mM DTT^{ox}, 20 mM Tris-HCl, 1 mM EDTA, 25 °C, for the control (○); (b) control + 4 μM PDI (□); (c) control + 4 μM null PDI (▲); (d) control + 4 μM ab (×); (e) control + 4 μM b′a′ (◇); and (f) control + 4 μM bb′ (Δ).

Separately, apo-ALAC was introduced into a folding buffer which contained either 1 mM DTT^{red} or 4 μM reduced wild-type PDI. The samples were processed and analyzed as above.

Gdn-HCl unfolded C65AC72A RNase A was introduced into folding conditions by dilution of 5 mg/mL C65AC72A RNase A (pH 8, 4 M Gdn-HCl, 100 mM Tris-HCl) into a folding buffer (100 mM Tris-HC, pH 8) such that the final Gdn-HCl concentration was 0.1 M (30 μM protein). In other experiments the folding buffer contained either 1 mM DTT^{red} or 4 μM reduced wild-type PDI instead of 1 mM DTT^{red}. The samples were processed and analyzed as above.

RESULTS

Regeneration of RNase A. The kinetic data pertaining to the regeneration of RNase A were fitted to a first-order rate equation, $\ln(1 - N) = -kt$, where $1 - N$ is the fractional concentration of all non-native species, k represents the rate constant for the formation of the native protein, and t is the reaction time (*20*). Figure 4 is a plot of the regeneration data of RNase A catalyzed by PDI and its subdomains. The data indicate that the regeneration rate is highest in the presence of WT PDI. For comparison, an uncatalyzed regeneration profile (control) is also included (○) and is in good agreement with previous reports (*18*). Table 1 summarizes the rate constants for the formation of the native protein as a function of PDI or any added domain. The oxidative folding rate of RNase A (50 mM DTT^{ox}, pH 8) is enhanced by the presence of composite ab and b′a′. At pH 8, an ∼2.1-fold increase in the rate of formation of the native protein is observed in the presence of ab (4 μM) whereas a 1.5-fold enhancement is induced by b′a′, compared to the control. These values are relatively low compared to catalysis by WT PDI (7.4-fold increase over the control). The addition of the hydrophobic bb′ did not impact, within error, the oxidative regeneration of RNase A (Table 1).

Measurement of the Impact of PDI on the Rate-Determining Step (3S → 3S) of RNase A Regeneration*. Table 2 lists the rate constants for the formation of 3S* species at pH 8 as a function of added domain. WT PDI catalyzed the formation of 3S* from its 3S ensemble by a factor of ∼11 over the control (−PDI). The individual domains had lesser catalytic efficiencies; the ab and b′a redox-active domains contributed approximately 2-fold over the rate observed in the uncatalyzed reaction. The bb′ domain does not appear to impact the reaction with respect to the control experiment.

Table 1: Regeneration of RNase A (50 mM DTT^{ox}, 100 mM Tris-HCl, 1 mM EDTA, 25 °C)

folding condition, pH 8	rate constant (pH 8) for R → N ($\times 10^4$ min^{-1})	catalytic impact (adjuvant/control)
R	11 ± 0.5	
R + 4 μM WT PDI	81.3 ± 0.4	7.4
R + 4 μM null PDI	11.2 ± 0.1	1.02
R + 4 μM ab	23 ± 0.3	2.1
R + 4 μM b′a′	16 ± 0.25	1.45
R + 4 μM bb′	10.3 ± 0.7	0.93

Table 2: Rate Constants for Formation of 3S* Species of RNase A from Their Unstructured 3S Isomers as a Function of Added PDI or PDI Domain (4 μM, pH 8, 100 mM Tris-HCl)

adjuvant	k_f[a] [3S → 3S*] (−PDI) ($\times 10^3$)	k_f(adjuvant)/k_f(control)
control	1.6 ± 0.2	
WT PDI	18 ± 0.7	11.25
null PDI	2.1 ± 0.4	1.3
ab	4 ± 1.3	2.5
b′a′	3.2 ± 0.3	2
bb′	1.75 ± 0.4	1.1

[a] min^{-1}.

Measurement of PDI and Mutant Variant Impact on the Structure-Forming Step of Disulfide Bond-Containing Proteins. Figure 5 depicts a typical HPLC chromatogram showing the formation of 3S* species and $3S_{non\text{-}native}$ from $3S_{native}$ (at a particular time along the reaction pathway, using des (65−72)). The peak labeled R corresponds to $3S_{non\text{-}native}$. This is because the applied reduction pulse converts unstructured intermediates to R (*21*). Table 3 summarizes the quantity of $3S_{native}$ species that conformationally folds to a stable intermediate (3S* species). Note: The results were identical whether des (65−72) or des (40−95) was used as the starting material. Hence, des (65−72) was used because the quantity in hand was larger than the quantity of des (40−95) that was available. In the absence of any added PDI or PDI subdomain, ∼32% of the $3S_{native}$ species is able to conformationally fold to the stable 3S* intermediate, in agreement with previously reported literature (*13*). The addition of WT PDI results in a large decrease in the amount of 3S* formed (8-fold over the control). Similarly, the rate of formation of 3S* by conformational folding of $3S_{native}$ is reduced addition of either ab or b′a′ composite domains, although their ability to reshuffle $3S_{native}$ to $3S_{non\text{-}native}$ is diminished relative to WT PDI. In contrast to these results, the addition of null PDI or the hydrophobic bb′ domain results in an enhanced conformational folding rate of the $3S_{native}$ species to 3S* relative to the control that lacks PDI (40% and 38%, respectively, relative to 32%).

Table 4 reports the refolding yield of ALAC in the presence of 1 mM DTT^{red} or 4 μM reduced wild-type PDI. The refolding yield obtained from the control experiment is also tabulated. The data indicate that the acquisition of the native fold (of ALAC) from its molten globule state is more effective in the presence of reducing conditions that are stronger than found in the ER milieu (1 mM DTT^{red}) than in the presence of PDI. It is noteworthy that the DTT^{red} concentration exceeds the oxidoreductase concentration by a factor of 250. A reduction of ∼30% in the formation of native ALAC by PDI is observed relative to the control.

Similarly, introduction of C65AC72A RNase A into folding conditions in the presence of 1 mM DTT^{red} results in its reduction (failure to form the native fold) compared to the control and

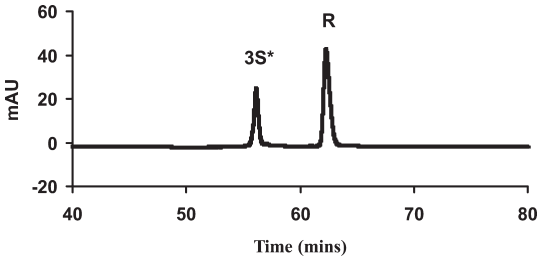

FIGURE 5: Typical reversed-phase HPLC chromatogram (C18 column) showing results of the competition between the structure-forming step ($3S_{native}$ → 3S*) and thiol−disulfide exchange reactions ($3S_{native}$ → $3S_{non\text{-}native}$). Any 3S* formed by the physical conformational folding reaction of $3S_{native}$ can easily be separated from the remainder of $3S_{native}$ that chemically reshuffles and isomerizes to form $3S_{non\text{-}native}$ and eventually populates all 419 unstructured isomers. This is possible by the application of a reduction pulse that reduces any unstructured intermediate (such as $3S_{non\text{-}native}$ and 419 isomers) to the fully reduced protein. Reversed-phase HPLC is then used to separate 3S* from R (formerly $3S_{non\text{-}native}$ and 419 unstructured isomers). The fraction of 3S* formed can then be quantified as described in Materials and Methods.

Table 3: Measurement of Oxidoreductase Impact on Structure-Forming Step of RNase A (pH 8, 100 mM Tris-HCl, 25 °C)

species	$3S_{non\text{-}native}$ (%)	3S* (%)
	68 ± 1.7	32 ± 1.4
WT PDI	96 ± 2.2	4 ± 1.2
null PDI	60 ± 0.7	40 ± 0.34
ab	81 ± 0.8	19 ± 1.9
b′a′	79 ± 0.67	21 ± 0.89
bb′	62 ± 2.3	38 ± 1.22

Table 4: Measurement of Oxidoreductase Impact on Structure-Forming Step in the Regeneration of ALAC and C65AC72A (pH 8, 100 mM Tris-HCl, 25 °C)[a]

protein	control	+1 mM DTT^{red}	+4 μM reduced PDI
ALAC	0.99 ± 0.01	0.97 ± 0.09	0.67 ± 0.04
C65AC72A	1.00 ± 0.02	0.96 ± 0.03	0.74 ± 0.07

[a] Values denote fraction of native protein formed from the unfolded state. The ALAC folding buffer contained 20 mM Ca^{2+}.

DTT^{red}-containing samples (Table 4). However, the presence of reduced wild-type PDI (4 μM) in the folding buffer resulted in a more severe reduction in the yield of native (fully refolded) C65AC72A RNase A (∼25% compared to the control).

DISCUSSION

In vivo, oxidative protein folding takes place within the oxidizing environment of the ER lumen (*4*). Within the ER environs, nature has invested in an oxidoreductase chaperone, protein disulfide isomerase (PDI), which facilitates rapid exchange between thiols and disulfides and catalyzes oxidative folding of "substrate" proteins (*15*, *23*, *24*).

However, during maturation of disulfide-containing proteins, the rate-determining step is often a composite process comprised of chemical and physical half-processes (*5*−*7*). Furthermore, the physical conformational folding reaction that is required for the generation of native (native-like) structure competes with thiol−disulfide exchange reactions (such as reduction and/or isomerization reactions) (Figure 2). The role of PDI in the pivotal conformational folding step, which inherently competes with thiol−disulfide exchange, has heretofore not been explored.

In this study, we have examined the impact of PDI and its domains on the rate-determining step in the regeneration of RNase A, with emphasis on dissecting its role in conformational folding of RNase A and other disulfide bond-containing proteins. Furthermore, we have also studied the role of null and domains ab, b′a′, and bb′ in the RDS of RNase A oxidative regeneration. The ab and b′a′ are composite in that they contain both redox-active and hydrophobic components and permit "overall" assessment of mixed domain contribution to the structure-coupled step; bb′ is a largely hydrophobic domain previously implicated in chaperone activity (*17*). This domain permits assessment of the contribution of the hydrophobic domain of PDI to the rate-determining and conformational folding steps.

The viability of each expressed domain was examined by evaluating its ability to regenerate fully reduced RNase A. Regeneration data of fully reduced RNase A (Table 1) indicate that both composite domains are catalytically active in agreement with previous studies (*19*). Null PDI and the hydrophobic bb′ domain do not significantly impact the overall oxidative folding rate at both pHs tested (Table 1). Taken together, the results obtained suggest that catalysis of redox reactions plays a greater role in facilitating oxidative folding than any "chaperone-like" activity.

The roles of WT PDI and subdomains in catalyzing the rate-determining step of RNase A regeneration were next examined. Since the formation of $3S_{native}$ is mandatory to conformational folding (species with non-native disulfides do not acquire stable tertiary structure (*5*)), a catalyst that can increase the frequency with which $3S_{native}$ forms from its unstructured isomers ($3S_{non\text{-}native}$) would catalyze the overall formation of 3S* from $3S_{non\text{-}native}$ (the RDS). The hydrophobic domains, along with null PDI, barely impact the RDS, suggesting that hydrophobic interactions do not play a significant role in the RDS.

To investigate the role played by PDI and its domains in the pivotal structure-forming step of the oxidative folding process, we first populated a RNase A transient three-disulfide intermediate containing only native disulfide bonds ($3S_{native}$) by pH denaturation of (native-like) structured RNase A intermediates, des [40−95] and des [65−72] (*13*). This technique results in the preservation of native disulfide bonds (by protonating cysteine sulfurs) while resulting in the denaturation of the native-like des species; i.e., 3S* is converted to $3S_{native}$ at low pH, and native disulfide bonds are prevented from becoming reshuffled through intramolecular thiol−disulfide exchange. Through this tool, the previously transient intermediate ($3S_{native}$) is now "frozen" and amenable to further experimentation. Similarly, through analogous chemical tools we were able to manipulate and trap ALAC and C65AC72A RNase A into states that are "poised to fold". This biochemical inroad is critical to deconvoluting the physical folding step from the chemical thiol−disulfide exchange step in the RDS of oxidative protein folding.

In the absence of any added PDI/subdomain, our data indicate that 30% of the $3S_{native}$ species conformationally folds to form structured (native-like) 3S* species (Table 3). The remainder back-reshuffles to $3S_{non\text{-}native}$ due to intramolecular attack by free cysteines on the native disulfide bonds before the conformational folding reaction can lock in the native disulfide bonds within stable tertiary structure. In the conformational folding of RNase A, proline isomerization is rate-limiting and hence back-reshuffling predominates (~70% of $3S_{native}$ is back-reshuffled to $3S_{non\text{-}native}$) (*10*, *13*). The addition of WT PDI results in a drastic decrease in the percentage of $3S_{native}$ that can undergo successful conformational folding to form 3S* (Table 3). This is because PDI cysteines accelerate the thiol−disulfide exchange between free cysteines of $3S_{native}$ and its native disulfide bonds and convert native bonds to non-native bonds. The PDI-facilitated thiol−disulfide exchange outcompetes the conformational folding of $3S_{native}$ to 3S*. Hence, a larger fraction of $3S_{native}$ is converted to $3S_{non\text{-}native}$ in the presence of PDI. The addition of null PDI or the hydrophobic bb′ domain results in a slightly improved conformational folding rate as evident from the percentage of 3S* formed (Table 3). This may be due to binding of the hydrophobic bb′ domain to the unstructured $3S_{native}$ species and stabilization of the unstructured intermediate in agreement with previous peptide binding data which suggest that the bb′ domains are able to bind to unstructured peptides (*17*). In conjunction with results obtained upon the addition of WT and null PDI, the addition of composite ab and b′a′ domains confirmed that the redox-active domains have a higher impact on back-reshuffling than the hydrophobic domain has on the forward rate, resulting in a net loss in formation of structured intermediates in the presence of PDI.

The impact of WT PDI on the structure-forming step of two other model proteins was also examined (Table 4). ALAC is a calcium-bound protein that collapses to a molten globule state upon removal of the Ca^{2+} ion (*22*). Conversely, acquisition of ALAC tertiary structure requires the presence of the metal ion. In the experimental setup, molten globule ALAC was introduced into a Ca^{2+}-containing buffer. Under these conditions, ALAC can conformationally fold. The reintroduction of Ca^{2+} in the presence of a reducing agent (1 mM DTT^{red}) resulted in the reduction of 2% of ALAC over the control experiment. It is noteworthy that DTT^{red} is a strong reducing agent compared to GSH; the data indicate that the conformational folding of ALAC was largely completed before the reduction of any disulfide bond could take place under conditions representing a relatively strong (compared to the ER) reducing environment. In contrast, the addition of only 4 μM reduced WT PDI resulted in the reduction of a nominal 2% of ALAC, suggesting that the potent oxidoreductase activity of PDI hampers the metal ion-induced structure-acquisition step in the ALAC folding pathway.

C65AC72A RNase A is a three disulfide bond-containing mutant RNase A that conformationally folds upon acquisition of its three native disulfide bonds (*10*). It mimics the folding pathway of hirudin and several other ER-processed proteins (*1*, *3*). The structure-coupled folding step of C65AC72A RNase A was mimicked by introducing the protein into unfolding conditions, followed by dilution into folding conditions. Similar to results observed in the metal ion-dependent folding scenario, the reduction of C65AC72A RNase A was more effective by fully reduced WT PDI (4 μM) than by a 250-fold excess of a strong reducing agent.

Importantly, our data demonstrate remarkable conflicting catalytic actions of PDI and its domains on the pivotal structure-forming step which precedes maturation of disulfide bond-containing proteins. Although WT PDI facilitates oxidative folding and catalyzes the RDS, by virtue of its redox-active domains it is highly detrimental to the forward folding reaction of those species that are poised to conformationally fold (viz., RNase A $3S_{native}$ species; ALAC molten globule and C65-AC72A RNase A). On the other hand, null PDI and the hydrophobic bb′ domains bestow chaperone-like conformational folding assistance during the structure-forming step (as seen in

RNase A $3S_{native}$ species) even though they do not have a significant effect on the overall regeneration rate and the RDS.

Notably, the highly evolved redox activity of PDI, finely tuned to catalyze the highly redox-dependent oxidative folding process, becomes self-limiting in the pivotal and mandatory conformational folding event in oxidative regeneration. It overwhelms the promotion of the forward reaction by the limited chaperone activity demonstrated by the hydrophobic domains. The impact of PDI on the various stages of oxidative folding is discussed, using the RNase A regeneration pathway as a model.

Previous data have shown that PDI accelerates oxidation and isomerization reactions along the regeneration pathway of ER-processed proteins (*15*, *16*, *18*). In this study, we demonstrate that the oxidoreductase activity of PDI is instrumental in accelerating the RDS of RNase A regeneration. However, we also observed that PDI hampers the conformational folding step, which forms the latter half of the RDS; i.e., the ~11-fold acceleration in the RDS includes an observed 8-fold inhibition in the formation of 3S* due to back-reshuffling of species that are poised to fold. The highly evolved oxidoreductase activity of PDI thus limits its full potential in catalyzing the RDS and the overall oxidative folding rate. In other model folding scenarios involving disulfide bond-containing proteins, the presence of PDI was again detrimental.

CONCLUSIONS

Protein traffic in the ER comprises incoming nascent chains that need to fold, outgoing bioactive polymers that constitute the secretory pathway, and terminally misfolded debris constituting the retrotranslocatory pathway. Efficient catalytic function of PDI is pivotal to directing the majority of incoming traffic along the secretory pathway. Compromised PDI activity can increase retrotranslocatory flux which in turn can overwhelm the cytosolic housekeeping machinery and lead to the onset of neuropathies (*25*, *26*).

Even under conditions of homeostasis, incoming substrates compete for PDI among themselves. This competition is in conflict with the tendency of substrates to aggregate and misfold. Reduced catalytic efficiency of PDI compromises its ability to process incoming proteins and direct them to the secretory pathway. Results from this study imply that the self-limited catalytic potential of PDI may detract a portion of the incoming flux from exiting the ER through the secretory pathway. Such a subset of the incoming flux would then constitute the retrotranslocatory pathway and impose on the cytosolic housekeeping machinery. The retrotranslocatory flux from the ER to the cytosol can thus set up conditions where aggregation-prone cytosolic proteins such as synphilin-1, synuclein, and Aβ escape surveillance by housekeeping leading to the onset of neuropathies such as Alzheimer's and Parkinson's diseases (*4*, *25*, *26*).

Nevertheless, other subcellular factors that may mitigate the detrimental impact of the oxidoreductase activity PDI during conformational folding include peptidyl prolyl isomerase which facilitates cis−trans isomerization of prolines (*4*). Thus, the presence of PPI is likely to accelerate formation of 3S* from $3S_{native}$ in those substrates whose conformational folding is limited by proline isomerization. Furthermore, competition for PDI's hydrophobic surface by a high concentration of unfolded substrate molecules in the ER, leading to detachment from PDI of $3S_{native}$, may also impact its deleterious isomerase activity during conformational folding.

Even though detailed studies need to be carried out to deconvolute the impact of individual factors before a general picture of the process of *in vivo* fold maturation becomes clear, our *in vitro* studies may have implications for understanding factors contributing to misfolding *in vivo*.

ACKNOWLEDGMENT

We thank Prof. Arni Holmgren and Dr. Alexios Vamos (Karolinska Institute, Sweden) for PDI plasmids and technical assistance with expression.

REFERENCES

1. Narayan, M., Welker, E., Wedemeyer, W. J., and Scheraga, H. A. (2000) Oxidative folding of proteins. *Acc. Chem. Res. 33*, 737–820.
2. Woycechowsky, K. J., and Raines, R. T. (2000) Native disulfide bond formation in proteins. *Curr. Opin. Chem. Biol. 4*, 533–539.
3. Arolas, J. L., Aviles, F. X., Chang, J. Y., and Ventura, S. (2006) Folding of small disulfide-rich proteins: clarifying the puzzle. *Trends Biochem. Sci. 31*, 292–301.
4. Tu, B. P., and Weissman, J. S. (2004) Oxidative protein folding in eukaryotes: mechanisms and consequences. *J. Cell. Biol. 164*, 341–346.
5. Wedemeyer, W. J., Welker, E., Narayan, M., and Scheraga, H. A. (2000) Disulfide bonds and protein folding. *Biochemistry 39*, 4207–4216.
6. Welker, E., Narayan, M., Wedemeyer, W. J., and Scheraga, H. A. (2001) Structural determinants of oxidative folding in proteins. *Proc. Natl. Acad. Sci. U.S.A. 98*, 2312–2316.
7. Welker, E., Wedemeyer, W. J., Narayan, M., and Scheraga, H. A. (2001) Coupling of conformational folding and disulfide-bond reactions in oxidative folding of proteins. *Biochemistry 40*, 9059–9064.
8. Rothwarf, D. M., and Scheraga, H. A. (1993) Regeneration of bovine pancreatic ribonuclease A. 1. Steady-state distribution. *Biochemistry 32*, 2671–2679.
9. Rothwarf, D. M., Li, Y. J., and Scheraga, H. A. (1998) Regeneration of bovine pancreatic ribonuclease A: identification of two nativelike three-disulfide intermediates involved in separate pathways. *Biochemistry 37*, 3760–3766.
10. Iwaoka, M., Wedemeyer, W. J., and Scheraga, H. A. (1999) Conformational unfolding studies of three-disulfide mutants of bovine pancreatic ribonuclease A and the coupling of proline isomerization to disulfide redox reactions. *Biochemistry 38*, 2805–2815.
11. Fink, M., Nieves, P., Chang, S., and Narayan, M. (2008) Non-redox-active small-molecules can accelerate oxidative protein folding by novel mechanisms. *Biophys. Chem. 132*, 104–109.
12. Wang, Y. H., and Narayan., M. (2008) pH dependence of the isomerase activity of protein disulfide isomerase: insights into its functional relevance. *Protein J. 27*, 181–185.
13. Saito, K., Welker, E., and Scheraga, H. A. (2001) Folding of a disulfide-bonded protein species with free thiol(s): competition between conformational folding and disulfide reshuffling in an intermediate of bovine pancreatic ribonuclease A. *Biochemistry 40*, 15002–15008.
14. Hawkins, H. C., and Freedman, R. B. (1991) The reactivities and ionization properties of the active-site dithiol groups of mammalian protein disulphide-isomerase. *Biochem. J. 275*, 335–339.
15. Weissman, J. S., and Kim, P. S. (1993) Efficient catalysis of disulphide bond rearrangements by protein disulphide isomerase. *Nature 365*, 185–188.
16. Wilkinson, B., and Gilbert, H. F. (2004) Protein disulfide isomerase. *Biochim. Biophys. Acta 1699*, 35–44.
17. Tian, G., Xiang, S., Noiva, R., Lennarz, W. J., and Schindelin, H. (2006) The crystal structure of yeast protein disulfide isomerase suggests cooperativity between its active sites. *Cell 124*, 61–73 Erratum: (2006) Cell *124*, 1085−1088.
18. Shin, H. C., and Scheraga, H. A. (2004) Catalysis of the oxidative folding of bovine pancreatic ribonuclease A by protein disulfide isomerase. *J. Mol. Biol. 300*, 995–1003.
19. Xiao, R., Wilkinson, B., Solovyov, A., Winther, J. R., Holmgren, A., Lundström-Ljung, J., and Gilbert., H. F. (2004) The contributions of protein disulfide isomerase and its homologues to oxidative protein folding in the yeast endoplasmic reticulum. *J. Biol. Chem. 279*, 49780–49786.

20. Xu, G., Narayan, M., and Scheraga, H. A. (2005) The oxidative folding rate of bovine pancreatic ribonuclease is enhanced by a covalently attached oligosaccharide. *Biochemistry 44*, 9817–9823.
21. Narayan, M., Welker, E., and Scheraga, H. A. (2003) Native conformational tendencies in unfolded polypeptides: development of a novel method to assess native conformational tendencies in the reduced forms of multiple disulfide-bonded proteins. *J. Am. Chem. Soc. 123*, 2909–2910.
22. Veprintsev, D. B., Permyakov, S. E., Permyakov, E. A., Rogov, V. V., Cawthern, K. M., and Berliner, L. J. (1997) Cooperative thermal transitions of bovine and human apo-alpha-lactalbumins: evidence for a new intermediate state. *FEBS Lett. 412*, 625–628.
23. Gilbert, H. F. (1998) Protein disulfide isomerase. *Methods Enzymol. 290*, 26–50.
24. Fewell, S. W., Travers, K. J., Weissman, J. S., and Brodsky, J. L. (2001) The action of molecular chaperones in the early secretory pathway. *Annu. Rev. Genet. 35*, 149–91.
25. Romisch, K. (2004) A cure for traffic jams: small molecule chaperones in the endoplasmic reticulum. *Traffic 5*, 815–820.
26. Romisch, K. (2005) Endoplasmic reticulum-associated degradation. *Annu. Rev. Cell Dev. Biol. 21*, 435–456.